Philosophical Transactions of the Royal Society of London Series A- Mathematical Physical and Engineering Sciences 360 (2002) 239-253

A novel strain sensor based on the campaniform sensillum of insects

A. Skordos, P. H. Chan, J. F. V. Vincent and G. Jeronimidis

Centre for Biomimetics, University of Reading, Whiteknights, Reading RG6 6AY, UK

Abstract

The functional design of the campaniform sensillum was modelled as a hole in a plate using two- and three-dimensional finite-element modelling. Different shapes of opening in a fibrous composite plate amplify differently the global strains imposed on the plate, and different configurations of reinforcement also have an effect. In this paper, the main objective is to study the strain and displacement fields associated with circular or elliptical openings in laminated plates in order to investigate their potential for integrated strain sensors. Since we are therefore primarily interested with the detection of displacement, the detailed stress concentration levels associated with these openings are not of primary concern. However, strain energy density levels associated with different hole and fibre configurations have been used to assess the relative likely strength reduction effect of the openings. To compare the relative strain amplification effect of drilled and formed holes of the same size in loaded plates, we have used the relative change in length of diameters (circular) or semi-axes (elliptical) in directions parallel and normal to the load.

Various techniques which could sense this deformation were investigated, in particular, the coupling mechanism of a campaniform sensillum of *Calliphora vicina*. This mechanism was resolved into discrete components: a cap surrounded by a collar, a joint membrane and an annulus-shaped socket septum with a spongy compliant zone. The coupling mechanism is a mechanical linkage which transforms the stimulus into two deformations in different directions: monoaxial transverse compression of the dendritic tip and vertical displacement of the cap. The mechanism is insensitive to change of the material properties of the socket septum, the cuticular cap and the spongy cuticle. The joint membrane may serve as a gap filler. The material properties of the collar have a substantial influence on the coupling mechanism's output. A 30% change of stiffness of the collar causes 45% change in the output of the coupling mechanism. The collar may be able to tune the sensitivity of the sensillum by changing its elastic properties.

Philosophical Transactions of the Royal Society of London Series A- Mathematical Physical and Engineering Sciences 360 (2002) 239-253

Keywords: hole; stress concentration; campaniform sensillum; fibrous composite; mechanical sensing; biomimetics

1. Introduction

Arthropod cuticle is a composite material made of chitin fibres in a matrix of crosslinked protein and other components. Stimuli caused by locomotion, posture and external events induce mechanical strains in the cuticle which have a rich variety of sensory information. This information is picked up by sensilla formed in the cuticle. Examples are the campaniform sensilla of insects and the slit sense organs of arachnids. We have investigated a sensillum modelled as a hole, round or oval, in a plate. The biological interest is in the integration of the sensilla with each other and the behaviour of the organism; the information technologist is interested in methods of encoding and transferring information; the engineer wants to design new sensing systems, possibly leading to novel embedded sensors which can be used for smart materials.

Physical models have commonly been used to explain and investigate the actions and mechanisms of the strain sensillum. For instance, Pringle (1938) constructed a model from a rubber sheet and a strip of paper to explain the mode of action of the sensillum. Slit sense organs in spiders were modelled in Plexiglas (Barth & Pickelmann 1975). However, owing to the complexity of sensillum it is extremely difficult, if not impossible, to make a physical model to represent its geometry as well as its constituent materials. As a result, simplifying assumptions have to be made in the geometry and the constituent materials of the physical model. We have used finite-element analysis to investigate the deformation of the hole which forms the sensing element of the sensillum, and the output of the coupling mechanism which is found in nature.

A hole is commonly regarded as weakening a load-bearing structure, since it can initiate failure. However, the deformation of a hole before failure can yield useful information about the loads imposed. The stress concentration effects of openings of various geometry in anisotropic materials have been investigated theoretically and experimentally mainly in relation to situations where the fibres terminate at the edge of the holes (Lekhnitskii 1968). A circular hole drilled in a sheet of unidirectional fibrous composite material, thereby breaking fibres, for example, produces a dangerously high stress concentration, with theoretical values up to a factor of 8 (Jones 1975),

depending on the anisotropy ratio. Other early work on stress concentrations associated with cut outs of different geometry has been reported by Rowlands *et al* . (1973, 1974), Daniel *et al* . (1973, 1974) and Tirosh & Berg (1974). Strain concentration factors, on the other hand, are seldom reported. Whitney *et al* . (1982) quote some results in quasi-isotropic boron–epoxy laminated plates with cut-out holes from a comparative study between birefringence, classical strain gauge measurements and theoretical or numerical modelling. The measured strain concentration factors at the edge of the opening at the 90° position from the load direction are 3.34 (circular hole), 2.39 (elliptical hole, ellipticity 2, long axis parallel to load), 6.60 (elliptical hole, ellipticity 2, short axis parallel to load). As one would expect, the elliptical hole with short axis parallel to the load gives the highest strain concentration; the magnitude of the associated stress concentration will increase to infinity as the ellipticity increases. Work on the stress and strain concentration effects in composite plates with 'formed' holes, where the fibres follow the contour of the opening (curvilinear fibre pattern) instead of terminating at the boundary, has also received some attention (Heller & Chiba 1973; Cooper 1972; Hyer & Charrette 1991). However, in these studies too the emphasis has been on stress concentration and strength or buckling resistance reduction rather than on local deformability of the region perturbed by the holes.

2. Two-dimensional model

The campaniform sensillum is basically an opening in the cuticle covered by membrane layers. The shape of the opening is generally oval and sometimes almost circular. Its long and short axes vary from 6 to 24 μm and from 2 to 5 μm, respectively (Pringle 1938; Gnatzy *et al* . 1987). The chitin microfibrils in the cuticle extend around the hole so that it is equivalent to a formed hole in a sheet of fibrous composite material. The control was a plate with no opening in it; the experimental systems were a plate with a single circular opening in the centre, a plate with an elliptical opening and major axis aligned parallel to the direction of loading and a plate with an elliptical opening and major axis normal to the direction of loading. The experimental and modelling work was carried out on plates 1.8 mm thick, 70 mm wide and 160 mm long with circular holes of 7.5 mm diameter and elliptical holes of major axis 7.5 mm and minor axis 3.75 mm. These dimensions were chosen after verification that the perturbation due to the selected size of openings did not reach the boundaries of the plate (infinite plate approximation). All the

plates were loaded up to 1000 N mm−1 for comparison. For the fibre orientation, two modelling approaches were followed. The first is based on the assumption that the presence of the hole does not affect the fibre orientation, i.e. the fibres are parallel to the *x*-axis even very close to the hole. This corresponds to the case of a hole drilled after manufacturing. In the second approach the presence of the hole alters the orientation so that the fibres follow the edge of the hole; this disturbance relaxes gradually towards the unidirectional case away from the hole. This corresponds to a hole which has been formed during manufacturing. The distribution of fibre orientation depends on the manufacturing route, and if this manufacturing route is appropriate it can be a design parameter. In this study the following orientation distribution, as expressed by the fibre angle relative to the to load axis, has been used:

$$\left.\begin{aligned} F(r,\theta) &= -0.3333\theta\frac{r}{r_o} + 1.3333\theta, \qquad r_o \le r \le 4r_o, \\ F(r,\theta) &= 0, \qquad\qquad\qquad\qquad 4r_o \le r, \end{aligned}\right\} \tag{2.1}$$

where r is the distance from the opening centre, r_o is the opening radius for a circular opening and the major half-axis for an elliptical opening, $F(r,\theta)$ is the orientation function and θ is given by the following expression:

$$\left.\begin{aligned} \theta &= 0.8333\varphi - 75\theta, \qquad 0 \le \varphi \le 180, \\ \theta &= 0.8333\varphi - 225, \qquad -180 \le \varphi < 0, \end{aligned}\right\} \tag{2.2}$$

where φ is the angular coordinate for a cylindrical system of coordinates originating from the centre of the opening. The following correspondence exists between the Cartesian coordinates of a point and the cylindrical coordinates used in (2.1) and (2.2):

$$\left.\begin{aligned} r &= \sqrt{(x-x_c)^2 + (y-y_c)^2}, \\ \varphi &= Ar\tan\left(\frac{y-y_c}{x-x_c}\right), \end{aligned}\right\} \tag{2.3}$$

where subscript ‘c’ refers to the centre of the system of coordinates. This orientation distribution means that, in the hole region, the fibre follows the hole boundary starting from 75° at a point along the load axis (*x*-axis) and decreases gradually to 0° as the direction normal to the load axis is approached (*y*-axis). This orientation behaviour relaxes gradually as the distance from the centre of the hole increases and vanishes at distances greater than two hole diameters.

The boundary conditions used were

(i) fixed displacement at zero in all directions at one side of the plate;

(ii) a uniformly distributed tensile and/or shear load at the other end.

Tensile loads ranged from -1000 N mm^{-1} to 1000 N mm^{-1} (the minus sign corresponds to compression) and shear loads ranged from 50 N mm^{-1} to 300 N mm^{-1}.

3. Three-dimensional model

The sensillum is composed of mechanical coupling, transduction and encoding mechanisms to transfer the environmental information to the insect's nervous system. The mechanical coupling mechanism transforms the stimulus into another form before sending it to the dendrite of the attached sensory cell, which acts as a transducer.

One of the campaniform sensilla pG4 (Gnatzy *et al* . 1987; Grunert & Gnatzy 1987) was selected for modelling. The campaniform sensillum pG4 is located at posterior side of the second leg (Gnatzy *et al* . 1987). It is possible to construct a three-dimensional model of pG4 using one cross-section because of its circular shape. The coupling mechanism of the campaniform sensillum of *C. vicina* is composed of five components: (1) a cap; (2) a collar; (3) a joint membrane; (4) a dome-shaped socket septum; (5) a spongy compliant zone.

The fine structure of the pG4 campaniform sensillum of *C. vicina* (Grunert & Gnatzy 1987) was scanned into a computer. The contours of different parts of the sensillum were extracted by picking points on the scanned image. The three-dimensional (3D) structure of the sensillum was created by rotating this cross-section about the axis which goes vertically through the centre of the sensillum. According to Saint-Venant's principle (Gere & Timoshenko 1991), end effects can be neglected at locations which are at least a width of the plate away from any concentrated load, or from the end of the plate. Therefore, a cuticular plate was added to produce a unidirectional stress field. Only a quarter of the sensillum was needed, due to symmetry. The sensillum and the cuticle plate were discretized into 5904 eight-node 3D hexahedral elements. Different mechanical properties were allocated to the components of the sensillum. All cuticular materials are assumed to be isotropic. Figure 1 shows the axonometric view of the 3D model.

The model was subjected to arbitrary tensile and compressive stresses of 3 MPa. The actual dimensions of the model are not critical for the comparative study for which it has been used. However, the proportions of the various parts were the same as in the real sensillum chosen to

generate the model. The stress is applied along the *z*-axis of the 3D model. The analysis was performed using MARC FEA software using a nonlinear option in order to take the geometrical changes into account. The calculation was performed in 12 incremental steps with the full Newton–Raphson algorithm. The geometric stiffness matrix was updated by the Lagrangian method.

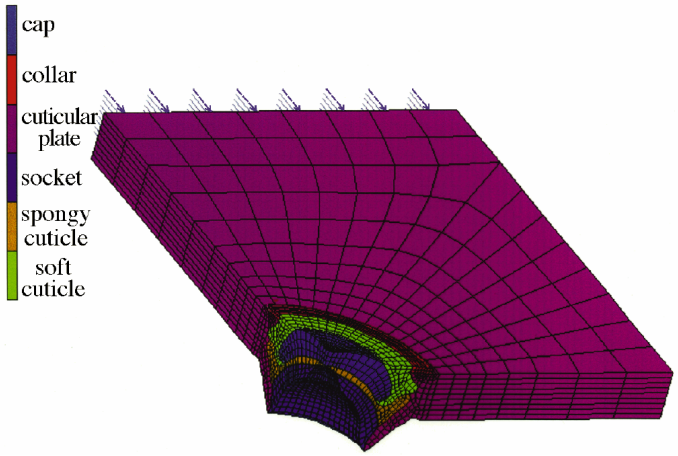

Figure 1. Axonometric view of the 3D finite-element model of the pG4 campaniform sensillum of Calliphora vicina. The stress is applied along the top edge (dotted arrows).

Table 1. Mechanical properties of the composite plate for 2D and 3D modelling

property	average	standard deviation
longitudinal modulus (MPa)	34600	2300
transverse modulus (MPa)	9100	450
in-plane shear modulus (MPa)	3700	50
major Poisson's ratio	0.31	0.05
minor Poisson's ratio	0.077	0.006

A simpler 3D finite-element model of a composite plate with a circular opening was also produced using anisotropic brick elements. This was done in order to compare experimental and modelling results. The dimensions of the plate and circular hole are the same as those of the 2D model. The plate comprised eight unidirectional glass–epoxy layers. The finite-element mesh was an extension of the mesh used to represent the composite plate with a circular hole in two dimensions, where each of the layers was represented by a layer of brick elements. The

mechanical properties of the elements were determined experimentally (table 1) from plates comprising eight layers of SE 84 HT (SP Systems) glass prepreg, uniaxially orientated, which had cured for 15 h at 80 ◦C. The final weight fraction of fibre was 69%. No additional results have been quoted for the 3D plate model because its in-plane behaviour was found to be virtually identical to that of the 2D model.

4. Results

(*a*) *Two-dimensional model*

For the chosen plate dimensions and opening sizes, the global stiffness of the fibre composite plates used in this study is not affected significantly by the presence of holes. At the selected maximum load of 1000 N mm−1 the average tensile strains in the load direction range from 2.85% (no opening) to 2.94% (circular formed hole), as shown in table 2. These strain values are high for a real system but since the problem is linear they can be scaled to more realistic levels. Plates with formed openings tend to have slightly higher compliance. Plates containing circular openings have a marginally higher compliance due to the fact that a circular opening with a diameter equal to the diameter of the major axis of an ellipse occupies a greater area of the plate. The changes in dimensions of the opening diameters parallel and normal to the loading were calculated as a percentage elongation or shrinkage. Results for the 1000 N mm^{-1} case are given in table 2. The analysis is linear elastic and all the simulations showed a linear dependence of the diametrical deformation on the applied load.

The openings amplify the local deformation up to eightfold, compared with the plate with no holes, and this is consistent with the reported result of the stress concentration in the vicinity of holes (Lekhnitskii 1968). The highest changes of dimension occur in the minor semi-axis of drilled (+19.3%) or formed (+15.8%) elliptical holes with major semi-axis normal to the load direction. In drilled holes the change of diameter or minor semi-axis parallel to the loading direction is higher than in formed holes for circular and elliptical holes with major semi-axis normal to the load. There is no significant difference of dimensional change in the major semi-axis between drilled and formed elliptical holes with major semi-axis parallel to the load direction. As the elliptical hole orientation changes from major semi-axis normal to parallel-to-the load, the local dimensional change in the load direction decreases, while that in the normal

direction increases. This effect is maximized in an elliptical opening oriented parallel to the loading, where the sensitivity of the normal axis becomes higher than the sensitivity of the parallel axis when a formed reinforcement configuration is used.

Table 2. Bulk elongation and compliance of the openings under 1000 N mm^{-1} tensile load

opening type	Bulk deformation	parallel to the loading	normal to the loading
no opening	2.85	2.87	−0.87
circular-drilled	2.91	11.90	−5.90
circular-formed	2.94	10.80	−9.44
elliptical-drilled major axis normal to load	2.90	19.30	−4.71
elliptical-formed major axis normal to load	2.92	15.81	−7.01
elliptical-drilled major axis parallel to load	2.87	7.43	−6.08
elliptical-formed major axis parallel to load	2.92	7.49	−12.77

The opening may induce failure. In our simplified model failure occurs when the strain energy density exceeds a value characteristic of the material. Thus, the strain energy distributions arising from the presence of openings can provide a first estimate of the strength reduction they cause (table 3). In the uniform plate the density is distributed uniformly across the plate except near the fixed boundary. This uniformity is disturbed by the presence of holes.

Table 3. Maximum strain energy density

opening type	maximum strain energy density (N mm$^{-2)}$
no opening	20.4
circular-drilled	221.5
circular-formed	93.9
normal elliptical drilled	453.7
normal elliptical formed	197.8
parallel elliptical drilled	94.6
parallel elliptical formed	52.1

The strain energy is maximum at an angle of 90◦ at the edge of the opening in all cases, except for the formed elliptical opening parallel to the loading where the maximum is located along the major axis of the ellipse. Drilled holes result in greater strain energy densities near the hole

boundaries and steeper gradients of its distribution in comparison with formed holes. In the worst case (elliptical drilled opening orientated normal to the direction of loading) the energy density increases twenty-fold compared with the intact plate. With formed holes the effect is not so pronounced; the strain energy maximum is reduced to about half that found with the drilled hole. This is illustrated by the way the strain energy concentration relaxes from its maximum close to the hole to a low value remote from the hole (figure 2*a, b*). The strain energy density is also distributed much more broadly across the specimen when the hole is formed rather than drilled. If the energy density at the worse position along the boundary of a hole is normalized relative to the maximum for the circular drilled hole, the various openings in table 4 can be ranked according to the severity of the local strain energy density to give: 1 (circular-drilled); 0.42 (circular-formed); 2.05 (elliptical-drilled major axis normal to load); 0.89 (elliptical-formed major axis normal to load); 0.43 (elliptical-drilled major axis parallel to load); 0.24 (elliptical-formed major axis parallel to load). The important result is that formed holes are typically half as severe as the drilled ones.

Table 4. The material properties of different parts in the coupling mechanism of the campaniform sensillum

	Young's modulus	Poisson's ratio
cuticular cap	6 GPa	0.3
cuticular collar	4.8 GPa	0.3
joint membrane	10 MPa	0.3
socket septum	0.15 GPa	0.3
spongy cuticle	2 MPa	0.3
cuticle	1.5 GPa	0.3

(*b*) *Three-dimensional model*

Initially each component of the model of the sensillum was given the same material properties to simulate the physical model approach using a homogeneous material. The Young's modulus of the body cuticle of *C. vicina* is about 1.5 GPa (Hepburn & Joffe 1976). The output of the coupling mechanism is indicated as the deformation of the dendrite of the attached sensory cell along three coordinate axes of the model. Figures 3, 4 and 5 show the output curve of the homogeneous model. The compressive stress is represented as a negative stress. Figure 3, which

indicates the vertical displacement of the cuticular cap, reveals that the cap indents under the tensile stress of the surroundings and bulges under the compressive stress. It also indicates that the compressive stress causes a transverse compression of the dendritic tip in the direction of the applied stress. The behaviour of the system appears to be very linear, a result which is perhaps not predictable *a priori* and interesting in its own right.

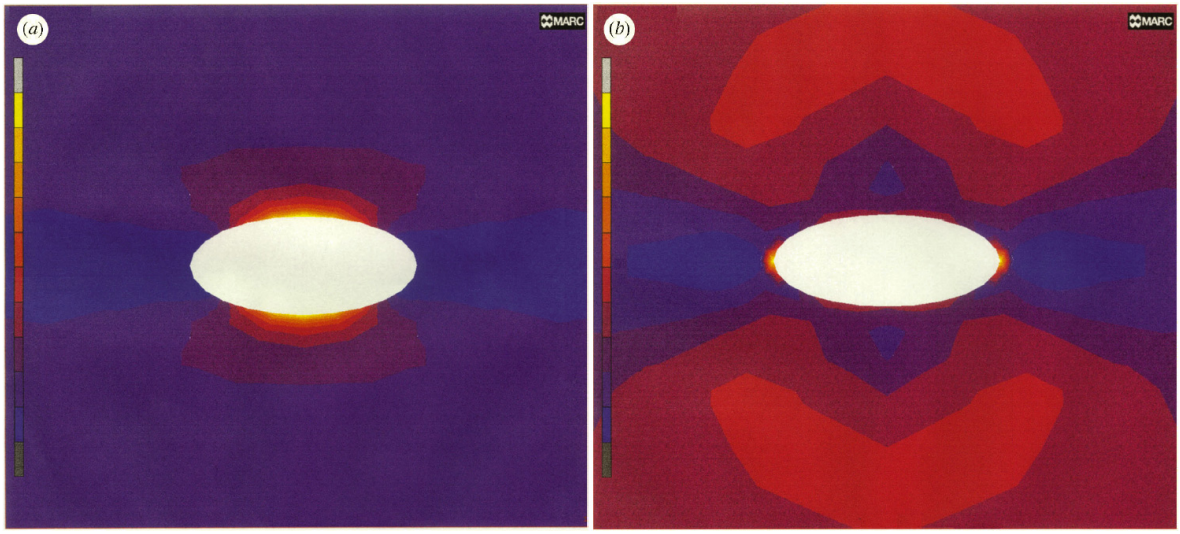

Figure 2. Strain energy distribution under tension in a plate with an elliptical opening orientated with its long axis parallel to the direction of loading. (a) drilled hole (left-hand scale ranges from 1 to 95 in 11 equal steps, higher values are lighter colours); (b) formed hole (left-hand scale ranges from 2 to 52 in 11 equal steps, higher values are lighter colours).

As far as we know the material properties of the pG4 campaniform sensillum have never been reported. Furthermore, there is a wide variation of material properties of the cuticle in a single animal. Therefore, we tried to infer the mechanical properties of the various cuticular elements of the coupling mechanism from their staining characteristics. The cuticular cap and upper parts of the cuticular collar do not stain and appear non-laminated. The lower region of the collar consists of laminate exocuticle. In transmission electron microscopy (TEM) the socket septum is seen to be fibrous. The cap and the collar therefore probably consist of relatively stiff tanned cuticle and the socket septum consists of relatively pliant cuticle. In TEM, the joint membrane appears to be homogeneous and is less electron-dense than the cuticle layers of the cap. The spongy cuticle, which appears transparent in TEM, probably consists of resilin (Jensen &Weis-Fogh 1962). The Young's modulus of sclerite cuticle of *C. vicina* (Hepburn & Joffe 1976) is also used in this

model. Tanned cuticle is more than three times stiffer than the untanned cuticle (Vincent 1990). Therefore, it is assumed that the Young's modulus of the heavily tanned cuticle is four times the Young's modulus of the sclerite cuticle. Although the cuticular collar comprises two different materials, it will be considered as a single material which is more pliant than tanned cuticle. The Young's modulus of resilin is consistent across various species at 2 MPa (Jensen & Weis-Fogh 1962). The stiffness of the joint membrane is regarded as between that of resilin and dry tanned cuticle. Its Young's modulus is assumed to be five times that of resilin. The modulus of the socket septum is assumed to be a tenth of sclerite cuticle due to its low fibre content. Table 4 summarizes the Young's modulus of the different components used in this model.

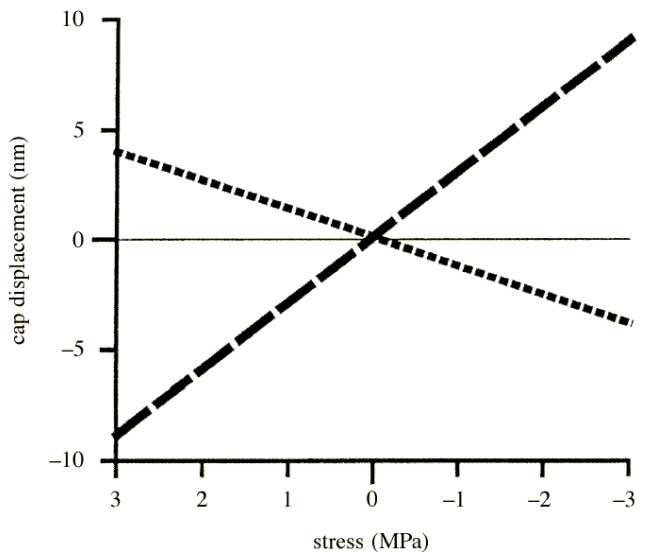

Figure 3. Output curves of the 3D finite-element of the entire sensillum. Indentation is represented model; short dashes, heterogeneous model.

The output curve of the heterogeneous model is also shown in figures 3, 4 and 5. The cuticular cap responds in an opposite way under some loading conditions. However, it acts the same as the homogeneous model in the other directions. The mechanical properties of the previous model were assigned according to the information available. These properties may differ from the real ones. Also the insect may vary the properties of the sensillum in different parts of its body in order to get mechanical matching between the sensillum and the surrounding cuticle. In order to investigate the effect of changes in the elastic properties of the elements on the output of the sensillum, a number of models were constructed. In each model, the stiffness of one of the components was changed from +30% to −30% of its ordinal value in steps of 10%. Each model

was then submitted to a compressive stress of 1 MPa. Only the vertical displacement of the cuticular cap is shown in this simulation (figure 6). The material properties of constituent materials affect the magnitude of the cuticular cap displacement (figure 7). However, all the models respond in the same way qualitatively.

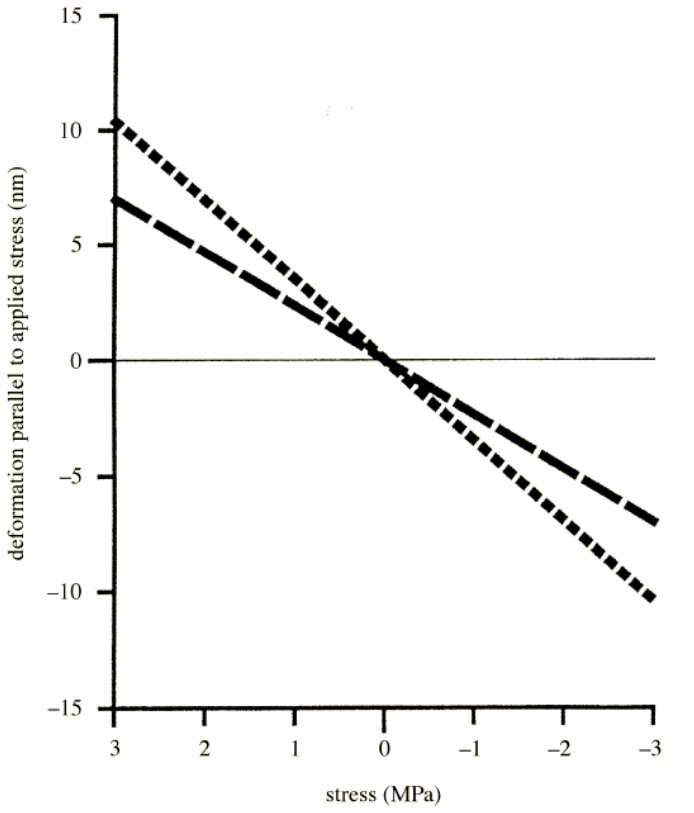

Figure 4. Output curves of the 3D finite-element model of the entire sensillum parallel to applied stress. Negative deformation means compression. Long dashes, homogeneous model; short dashes, heterogeneous model.

In the flat plate model, the distributions of stress and strain showed behaviour similar to that indicated by the 2D models. A large tensile stress developed normal to the loading at the two diametrical points on the boundary of the circular opening at mid-width under compression. This appears to be a weak point, as the transverse strength of a unidirectional glass/epoxy composite is expected to be very low. This effect is more intense along the major axis of an elliptical hole (figure 2*b*) as the stress concentration is higher in that case.

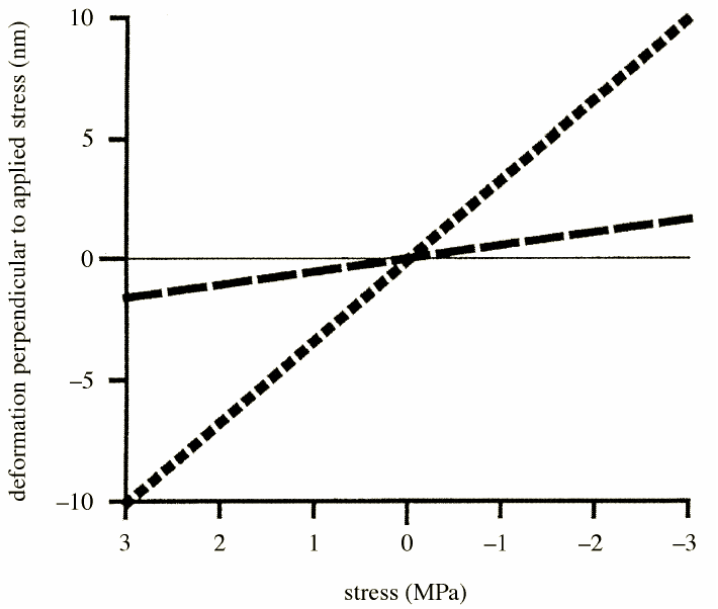

Figure 5. Output curves of the 3D finite-element model of the entire sensillum perpendicular to applied stress. Negative deformation means compression. Long dashes, homogeneous model; short dashes, heterogeneous model.

A way to overcome this problem is to modify the laying sequence of the composite. The internal layers of the laminate are subject to a lower, in comparison to the unidirectional case, normal to the loading tensile stress. Thus, a cross-ply laminate is expected to have a more acceptable strength under compression. Naturally, a crossply laminate will decrease the anisotropy of the sensing plate and consequently the strain amplification effects. However, the operating range of the strain sensor will be extended without having to use a thicker sensing plate to carry the service loads.

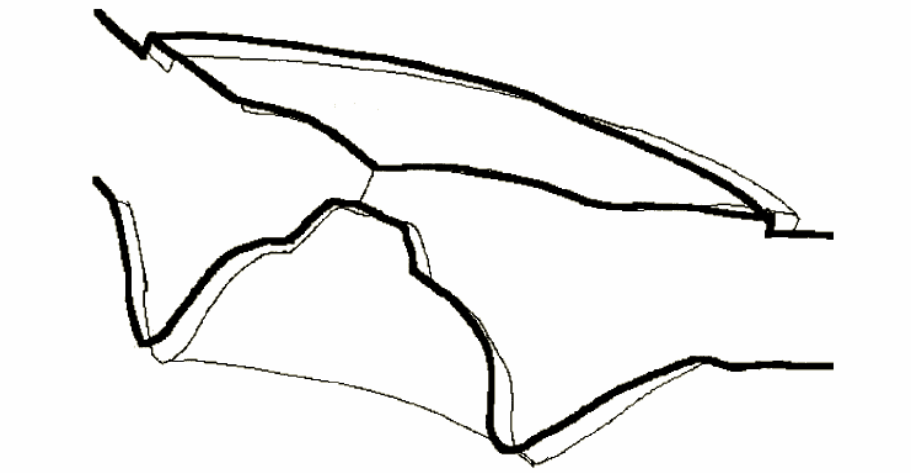

Figure 6. The deformation of the heterogeneous model under compressive stress. The heavy outline shows the undeformed model. The stress is applied in the Z-direction. The deformation is magnified ×25.

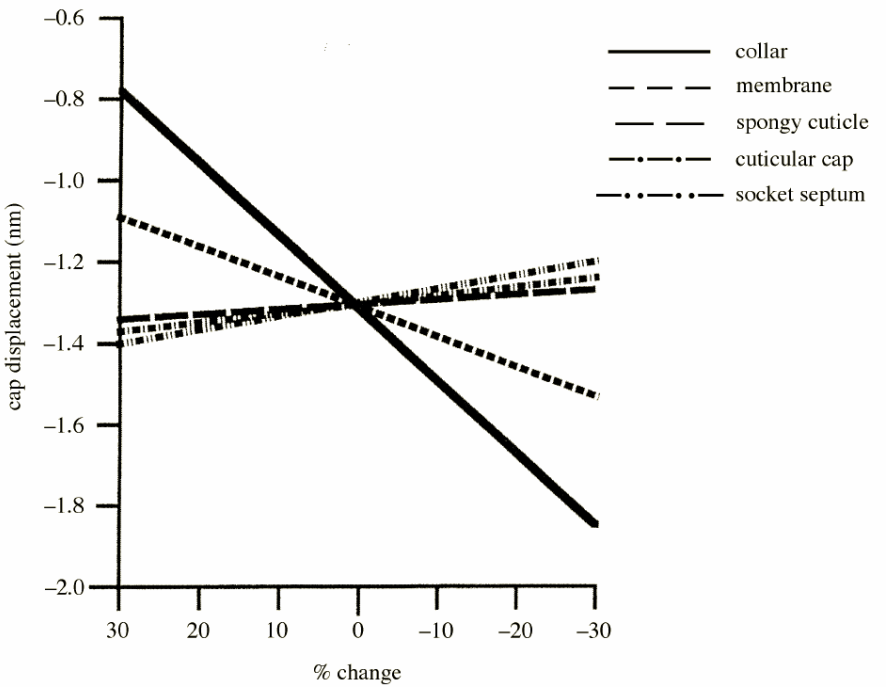

Figure 7. The response of the heterogeneous model, showing the effect of changing the stiffness of individual elements. Solid line, collar; short dash, membrane; long dash, spongy cuticle; dash-dot-dash, cuticular cap; dash-dot-dot-dash, socket septum.

5. Discussion

The results from the model with homogeneous material differ from the model with heterogeneous material. The cap of the homogeneous model moves in the opposite direction to the cap of the heterogeneous model under tensile and compressive stress of the main sheet of cuticle (figure 3). Furthermore, the magnitude of output of the heterogeneous model is larger than that of the homogeneous model in other two directions (figures 4 and 5). The material properties of constituent materials influence the output of the sensillum (figure 7). Therefore, the result of the physical model made of homogeneous material should be interpreted with caution since it is error

prone. The output of the coupling mechanism of the campaniform sensillum is insensitive to change of the stiffness of the socket septum, the cuticular cap and the spongy cuticle (figure 7). A 30% change in these stiffnesses causes only *ca*. 5% change in the output of the coupling mechanism. If the joint membrane is a stimulus transferring component, the change of output will be equal to or greater than the change of stiffness of the joint membrane. A larger stimulus can be transferred into the coupling mechanism when the stiffness of the joint membrane increases. However, the output of the coupling mechanism alters by 15% after a 30% change of the stiffness of the joint membrane. This suggests that the joint membrane is not a stimulus-transferring component. The joint membrane may serve as a gap-filler.

A 30% change of stiffness of the collar causes a 45% change of the output of the coupling mechanism; i.e. the change is amplified by 1.5 times. The collar consists of two parts: tanned cuticle in the upper region and laminated exocuticle in the lower part. The elastic properties of the collar can be altered by changing the thickness of tanned cuticle of the collar. Therefore, we speculate that the collar can tune the sensitivity of sensillum by changing its material properties. Further investigation is required to prove this hypothesis.

Thurm *et al* . (1975) conducted an electrophysiological and electromicroscopical study of the directional relation between stimulating deformations of the campaniform sensilla, which occur as a sensillum field at the base of the fly haltere, and the axes of this dendritic terminal. They deduced that stimulus increases the radius of the cuticular base plane by flattening the sensillum field. In turn, the width of the clefts between the arch-shaped collars is reduced by folding of the epicuticular joint membrane and compression of the space beneath. As a consequence, the tip of dendritic terminal is compressed by the socket septum transversely to its flat sides. Spinola & Chapman (1975) found that one of their ‘group 6’ campaniform sensilla on the cockroach tibia was stimulated by combinations of proprioceptive and punctuate stimuli. They inferred that the proprioceptive force indents the cap of the sensillum. They also suggested that the cap amplifies the cuticular strain to squeeze the tip of the dendritic sensory process.

The deformation of the heterogeneous model under compressive stress is shown in figure 6. It is assumed in this investigation that the proprioceptive force is a compressive stress and that the dendritic tip is squeezed in the direction of the applied stress field. On the other hand, no notable compression of the dendritic tip is shown in the direction perpendicular to the applied stress field. The proprioception indents the cap of model with constructed with heterogeneous materials. This

result agrees with Spinola & Chapman (1975). Some researchers (Spinola & Chapman 1975; Moran *et al* . 1976) suggest that the structure of the cap mechanically amplifies the cuticular strain to squeeze the tip of the dendritic sensory process. We cannot show amplification because our input data are qualitative. However, we can say that the coupling mechanism of the pG4 campaniform sensillum of *C. vicina* acts as a mechanical linkage which transform the applied force into two deformations in different direction. The deformation in the plane of the applied stress is more than twice the vertical deformation (comparing figures 3 and 4). The major excitatory deformation appears to be the compression of the dendritic tip parallel to the proprioceptive force. Although the vertical cap displacement may be a side effect produced by proprioceptive stimulation, the role of such displacement needs further investigation before a firm conclusion can be drawn.

Table 5. Potential sensing systems

	advantages	disadvantages
dome	further amplification of strain out of plane sensing	continuous sensing but needs a sensing element
optical techniques (photoelasticity, interferometry)	remote sensing potential for 'tell-tale' sensing	implementation difficulties
Resistance measurement	high accuracy	continuous sensing need to attach a resistor
piezoelectricity	good performance under dynamic loading	no static response continuous sensing
capacitance/impedance measurement	'tell-tale' measurement	continuous sensing need to attach a capacitor

In a simple finite-element model of the sensillum (which was supported by experiments, not reported here, on physical models), significant amplification of a global displacement in a composite plate can be achieved by introducing an opening in the plate. The shape of the opening and the arrangement of reinforcement around it can be widely varied offering a high degree of

flexibility for the design of a strain monitoring system. For example, when maximum amplification is required and the operational life of the sensing plate is not important, a drilled elliptical opening oriented vertically to the applied load can be used in order to achieve an amplification of the measured deformation by a factor of eight. In contrast, when the operational life of the sensing plate plays a role in the design, a formed elliptical hole will offer lower but still significant amplification accompanied by higher strength. In any case the sensing plate design can be optimized in a way that will combine both the strain amplification and strength requirements of a specific application.

A variety of solutions exists for the realization of sensing of the diametrical deformations (table 5). The use of a paste material enables the sensing device to store the maximum deformation. Such a technique offers the advantage of automated 'telltale' sensing at low cost. More sophisticated solutions involving the combination of conventional strain monitoring techniques with an appropriate electronic circuit can offer the ability to store information, combined with high accuracy.

A sensing system based on the use of a fibrous composite offers great flexibility, which can result in a wide range of designs. Such a sensing system can be tailored to the deformation amplification, strength and measurement output requirements of specific applications.

This study was supported by a Realizing Our Potential Award from EPSRC (ref. GR/K63054) and a contract from Technical Management Concepts, USA (ref. F33615-96-D5835). We thank Professor U. Thurm for his comments on an earlier draft and for providing an English translation
of part of his publication.

References

Barth, F. G. & Pickelmann, P. 1975 Lyriform slit sense organs: modelling an arthropod mechanoreceptor. *J. Comp. Physiol.* A103, 39–54.

Cooper, A. A. G. 1972 Trajectory fiber reinforcement of composite structures. PhD dissertation, Washington University, St Louis, MO, USA.

Daniel, I. M., Rowlands, R. E. & Whiteside, J. B. 1973 Deformation and failure of a boron–epoxy plate with circular hole. In *Analysis of the test methods for high modulus fibers and composites* (American Society for Testing Materials special publication 521), pp. 143–164.

Daniel, I. M., Rowlands, R. E. & Whiteside, J. B. 1974 Effects of material and stacking sequence on behavior of composite plates with holes. *Exp. Mech.* 14, 1–9.

Gere, J. M. & Timoshenko, S. P. 1991 *Mechanics of materials*, 3rd edn. London: Chapman & Hall.

Gnatzy, W., Grunert, U. & Bender, M. 1987 Campaniform sensilla of *Calliphora vicina* (Insecta, Diptera). I. Topography. *Zoomorphology* 106, 312–319.

Grunert, U. & Gnatzy, W. 1987 Campaniform sensilla of *Calliphora vicina* (Insecta, Diptera). II. Typology. *Zoomorphology* 106, 320–328.

Heller, R. A. & Chiba, T. 1973 Alleviation of the stress concentration with analogue reinforcement. *Exp. Mech.* 13, 519–525.

Hepburn, H. R. & Joffe, I. 1976 On the material properties of insect exoskeletons. In *The insect integument* (ed. H. R. Hepburn), pp. 207–235. Elsevier.

Hyer, M. W. & Charrette, R. F. 1991 Use of curvilinear fiber format in composite structuresdesign. *AIAA J.* 29, 1011–1015.

Jensen, M. & Weis-Fogh, T. 1962 Biology and physics of locust flight. V. Strength and elasticity of locust cuticle. *Phil. Trans. R. Soc. Lond.* B245, 137–169.

Jones, R. M. 1975 *Mechanics of composite materials*. Tokyo: McGraw-Hill Kogakusha.

Lekhnitskii, S. G. 1968 *Anisotropic plates*. New York: Gordon & Breach.

Moran, D. T., Rowley, J. C. & Zill, S. N. 1976 The mechanism of sensory transduction in a mechanoreceptor. *J. Cell Biol.* 71, 832–847.

Pringle, J. W. S. 1938 Proprioception in insects. II. The action of the campaniform sensilla on the leg. *J. Exp. Biol.* 15, 114–131.

Rowlands, R. E., Daniel, I. M. & Whiteside, J. B. 1973 Stress and failure analysis of a glass–epoxy plate with circular hole. *Exp. Mech.* 13, 31–37.

Rowlands, R. E., Daniel, I. M. & Whiteside, J. B. 1974 Geometric and loading effects on strength of composites plates with cutouts. In *Composite materials: testing and design* (American Society for Testing Materials special publication 546), pp. 361–375.

Spinola, S. M. & Chapman, K. M. 1975 Proprioceptive indentation of the campaniform sensilla of cockroach legs. *J. Comp. Physiol.* A96, 257–272.

Thurm, U., Stedtler, A. & Foelix, R. 1975 Reizwirksame Verformungen der Terminalstrukturen eines Mechanorezeptors. *Verh. Dtsch. Ges. Zool.* 67, 37–41.

Tirosh, J. & Berg, C. A. 1974 Experimental stress intensity factor measurements in orthotropic plates. In *Composite materials: testing and design* (American Society for Testing Materials special publication 546), pp. 663–673.

Vincent, J. F. V. 1990 *Structural biomaterials*, revised edn. Princeton, NJ: Princeton University Press.

Whitney, J. M., Daniel, I. M. & Pipes, R. B. 1982 *Experimental mechanics of fiber reinforced composite materials*. Brookfield Center, OH: Society for Experimental Stress Analysis.

https://dspace.org/

A novel strain sensor based on the campaniform sensillum of insects.

Skordos, Alexandros A.; Chan, P. H.; Vincent, Julian F. V.; Jeronimidis, G.

2002-02-01T00:00:00Z
Royal Society
http://dx.doi.org/10.1098/rsta.2001.0929
A. Skordos, P. H. Chan, J. F. V. Vincent and G. Jeronimidis; A novel strain sensor based on the campaniform sensillum of insects, Philosophical Transactions of the Royal Society of London Series A- Mathematical Physical and Engineering Sciences Vol 360 (2002) No1791 p239-253

Downloaded from a DSpace repository. https://dspace.org/